

Finite-Size Scaling in the Energy-Entropy Plane for the 2D $\pm J$ Ising Spin Glass

Ronald Fisch*
 382 Willowbrook Dr.
 North Brunswick, NJ 08902
 (Dated: June 28, 2018)

For $L \times L$ square lattices with $L \leq 20$ the 2D Ising spin glass with $+1$ and -1 bonds is found to have a strong correlation between the energy and the entropy of its ground states. A fit to the data gives the result that each additional broken bond in the ground state of a particular sample of random bonds increases the ground state degeneracy by approximately a factor of $10/3$. For $x = 0.5$ (where x is the fraction of negative bonds), over this range of L , the characteristic entropy defined by the energy-entropy correlation scales with size as $L^{1.78(2)}$. Anomalous scaling is not found for the characteristic energy, which essentially scales as L^2 . When $x = 0.25$, a crossover to L^2 scaling of the entropy is seen near $L = 12$. The results found here suggest a natural mechanism for the unusual behavior of the low temperature specific heat of this model, and illustrate the dangers of extrapolating from small L .

I. INTRODUCTION

The Edwards-Anderson (EA) spin glass¹ has been studied extensively for thirty years. A complete understanding of its behavior in two and three dimensions remains elusive. In recent years it has become possible to compute the free energy of the two-dimensional (2D) Ising spin glass with $\pm J$ bonds on $L \times L$ lattices with L of 100 or more.^{2,3,4,5,6,7} From these calculations on large lattices we have learned that extrapolations of data from lattices with $L < 30$ are often misleading.^{8,9,10,11,12}

A better understanding of why this happens is clearly desirable. This is especially true because essentially all of the work on three-dimensional (3D) EA models at low temperatures must be done on lattices with $L \leq 20$, due to our inability to equilibrate larger lattices at low temperatures in 3D.¹³ At least one example of complex behavior of the order parameter emerging as L is increased is already known in a similar 3D model.¹⁴

In this work we will analyze data for the energies and entropies of the ground states (GS) of 2D Ising spin glasses obtained using methods from earlier work.^{8,9,15} We will demonstrate that for small square lattices the $\pm J$ EA model has a strong correlation of the sample-to-sample fluctuations of the energy and the entropy of the GS. The increase of GS entropy S_0 with GS energy E_0 is too large to be explained by fluctuations in the number of zero-energy single-spin flips. This correlation may be the cause of the breakdown of naive scaling behavior at small L in this model.

II. THE MODEL

The Hamiltonian of the EA model for Ising spins is

$$H = - \sum_{\langle ij \rangle} J_{ij} S_i S_j, \quad (1)$$

where each spin S_i is a dynamical variable which has two allowed states, $+1$ and -1 . The $\langle ij \rangle$ indicates a sum

over nearest neighbors on a simple square lattice of size $L \times L$. We choose each bond J_{ij} to be an independent identically distributed quenched random variable, with the probability distribution

$$P(J_{ij}) = x\delta(J_{ij} + 1) + (1 - x)\delta(J_{ij} - 1), \quad (2)$$

so that we actually set $J = 1$, as usual.

The data analyzed here used an ensemble in which, for a given value of x , every $L \times L$ random lattice sample had exactly $(1 - x)L^2$ positive bonds and xL^2 negative bonds. Details of the methods used to calculate E_0 and the numbers of GS have been described earlier.¹⁵ S_0 is defined as the natural logarithm of the number of ground states. For each sample, E_0 and S_0 were calculated for the four combinations of periodic (P) and antiperiodic (A) toroidal boundary conditions along each of the two axes of the square lattice.¹⁵ We will refer to these as PP, PA, AP and AA. We use ALL to refer to a data set which includes the results from all four types of boundary conditions. In the spin-glass region of the phase diagram, the variation of the sample properties for changes of the boundary conditions is small compared to the variation between different samples of the same size,⁹ except when x is close to the ferromagnetic phase boundary and the ferromagnetic correlation length becomes comparable to L .

III. GROUND STATE PROPERTIES

The average GS entropy $\langle S_0 \rangle$ of an $L \times L$ sample for this model is essentially proportional to L^2 , the number of spins, with a small finite-size correction.¹⁵ It was discovered earlier,¹⁵ however, that for $x = 0.5$ the ratio of the width of the distribution of S_0 for different samples of size L divided by $\langle S_0 \rangle$ is not a monotonic function of L , having a peak at $L = 8$. A similar change in behavior between $L = 8$ and $L = 10$ was seen earlier by Saul and Kardar in samples with open boundary conditions, and appears in Fig. 11 of their paper.⁹ The original motivation of the current study was to understand the origin of

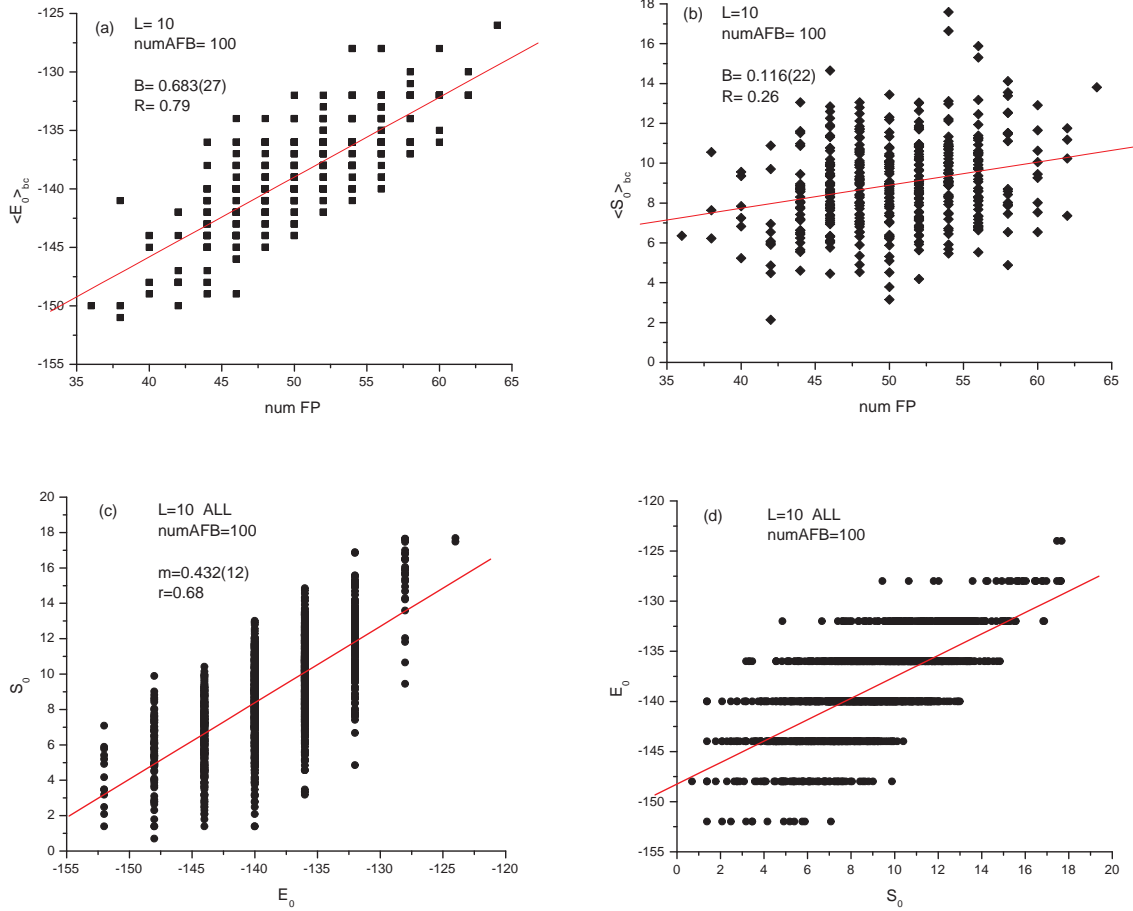


FIG. 1: (color online) Scatter plots of correlations for $x = 0.5$ and $L = 10$: (a) E_0 averaged over boundary conditions vs. number of frustrated plaquettes; (b) S_0 averaged over boundary conditions vs. number of frustrated plaquettes; (c) S_0 vs. E_0 ; (d) E_0 vs. S_0 . The number of samples used is 400, and the lines through the data are least-squares fits.

this unexpected behavior. Our ensemble, unlike the one used by Saul and Kardar, does not keep the number of frustrated plaquettes fixed.

We first look to see if the GS properties are correlated with the number of frustrated plaquettes, with the number of bonds of each type held fixed. The scatter-plot data for $x = 0.5$ and $L = 10$ are shown in Fig. 1(a). There is a substantial correlation of E_0 with the number of frustrated plaquettes, and this correlation seems to be independent of L . Since it is well known that E_0 increases as the number of frustrated plaquettes is increased, this is expected.

There is a weaker correlation between S_0 and the number of frustrated plaquettes, as shown in Fig. 1(b). On the average, increasing the number of frustrated plaquettes increases S_0 . This correlation is also not surprising, since positive S_0 arises from rearranging the strings of broken bonds which connect the frustrated plaquettes in a GS. It seems natural that a larger number of frustrated plaquettes would give a larger number of ways to rear-

range the strings of broken bonds.

For Fig. 1(a) and 1(b), we have averaged E_0 and S_0 over the four different boundary conditions for each sample, because the number of frustrated plaquettes does not depend on the boundary conditions. In the remainder of this work, we will treat each boundary condition for each sample independently.

All equilibrium statistical mechanics can be derived from the partition function, which is determined by the energy and the entropy. Therefore, we would like to know if E_0 and S_0 are correlated with each other. The scatter plots for this correlation from the same data are shown in Fig. 1(c), along with a least-squares fit to the data, treating E_0 as the independent variable. Fig. 1(d) shows the same data with the roles of energy and entropy reversed. It demonstrates that the least-squares fit depends on which variable is chosen as the independent one.

The results of least-squares fits for $x = 0.5, 0.25$ and 0.125 , and L varying from 6 to 20 are shown in Figures 2, 3 and 4, respectively. For each value of x and each L ,

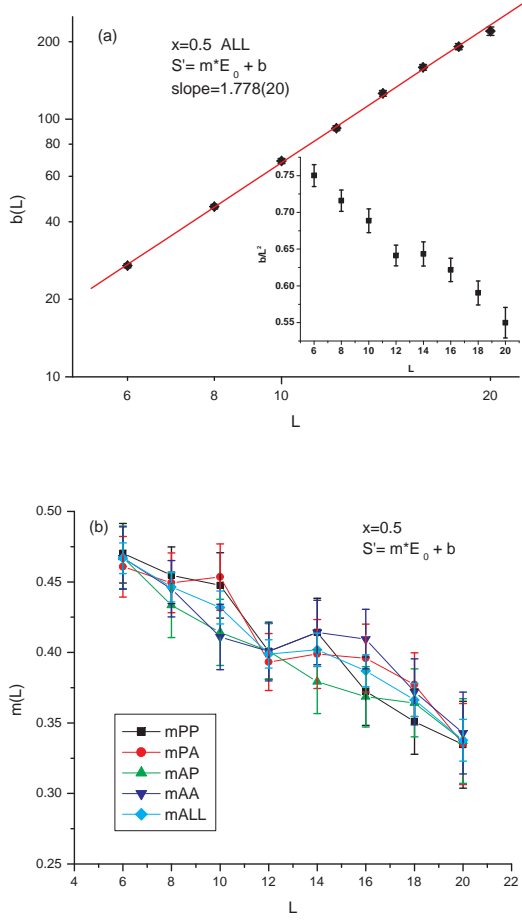


FIG. 2: (color online) Results of least-squares fit analysis parameterized by Eqn. (3) of the scatter plot of correlations between E_0 and S_0 for $x = 0.5$: (a) b vs. L , log-log plot; inset: b/L^2 vs. L ; (b) m vs. L . The number of samples used for each L , ($L, \#$), is (6:400), (8:400), (10:400), (12:400), (14:400), (16:400), (18:400) and (20:238).

we show the slope m given by the least-squares fit, and the offset b of the entropy, defined by

$$S'(E_0) = m * E_0 + b. \quad (3)$$

S' is the dependent variable in the least-squares fit. Note that E_0 is negative.

In Figures 5, 6 and 7, we give the value of r , the normalized covariance defined by

$$r(E_0, S_0) = \frac{\langle E_0 S_0 \rangle - \langle E_0 \rangle \langle S_0 \rangle}{\sigma(E_0) \sigma(S_0)}, \quad (4)$$

for each fit. The angle brackets indicate an average over the random bond distribution for some fixed value of x . The standard deviation, σ , is defined, as usual, as

$$\sigma(X) = \sqrt{\langle X^2 \rangle - \langle X \rangle^2}. \quad (5)$$

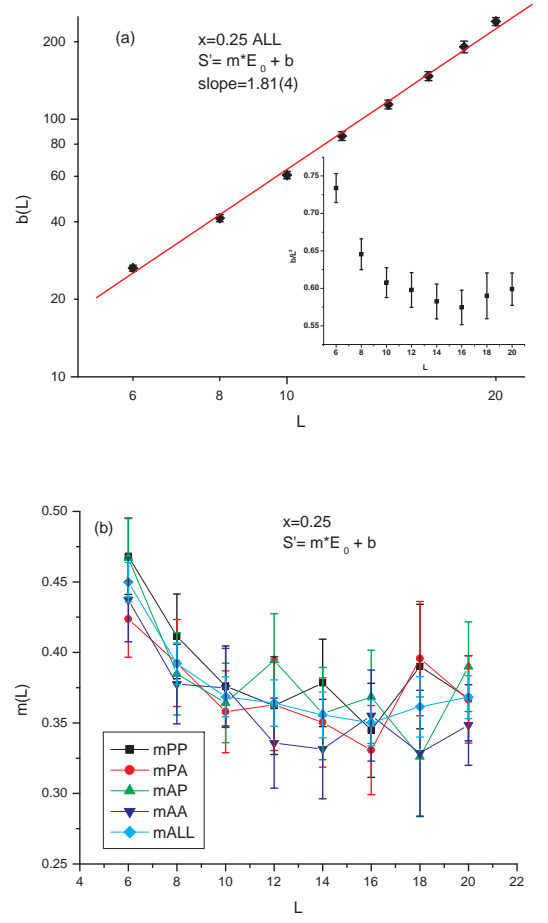


FIG. 3: (color online) Results of least-squares fit analysis parameterized by Eqn. (3) of the scatter plot of correlations between E_0 and S_0 for $x = 0.25$: (a) b vs. L , log-log plot; inset: b/L^2 vs. L ; (b) m vs. L . The number of samples used for each L , ($L, \#$), is (6:200), (8:200), (10:200), (12:200), (14:200), (16:200), (18:133) and (20:200).

The numbers in parentheses and the error bars shown in the figures represent a one standard deviation statistical error, as calculated by the Origin 6.0 Professional¹⁷ least-squares fitting routine. One expects that, in addition, there may be systematic errors arising from non-ideal behavior of random number generators and nonlinear correlations. It is often difficult to obtain meaningful estimates of systematic errors.

For small L there is a strong correlation between E_0 and S_0 . As L increases, $\sigma(E_0)$ increases linearly with L but $\sigma(S_0)$ increases faster than linearly over this range of L . Thus the correlation gets weaker as L increases. This is reflected in the tendency for r to decrease as L increases. From our data, it is not clear whether or not r goes to zero as L goes to infinity. It is generally believed that the model is not self-averaging at $T = 0$, so it would be natural for r to remain finite as L increases.

The value of r depends on the choice of ensemble. For

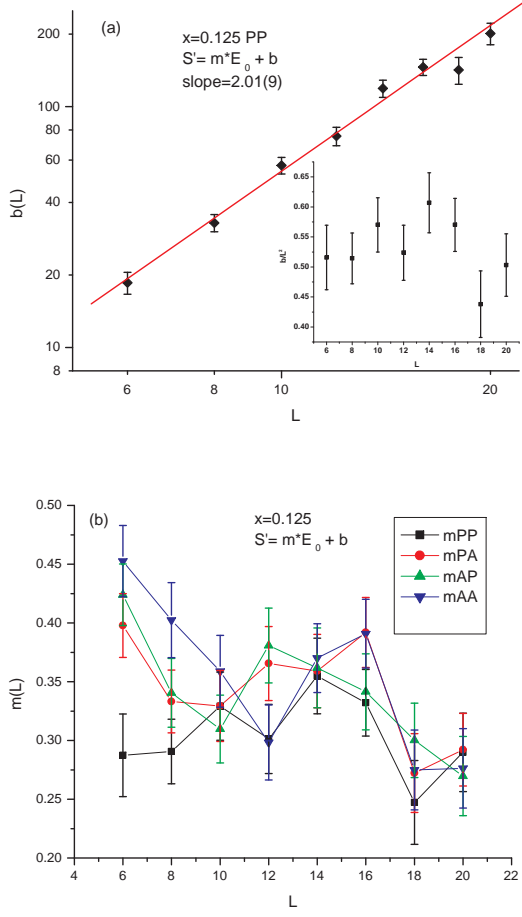


FIG. 4: (color online) Results of least-squares fit analysis parameterized by Eqn. (3) of the scatter plot of correlations between E_0 and S_0 for $x = 0.125$: (a) b vs. L , log-log plot; inset: b/L^2 vs. L ; (b) m vs. L . The number of samples used for each L , ($L, \#$), is (6:200), (8:200), (10:200), (12:200), (14:200), (16:200), (18:200) and (20:200).

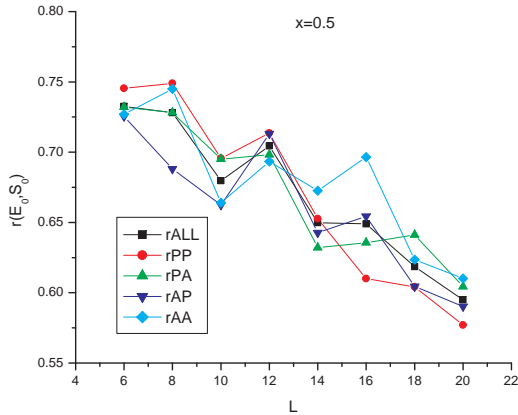


FIG. 5: (color online) Covariance of ground state energy and ground state entropy, $r(E_0, S_0)$ vs. L for $x = 0.5$.

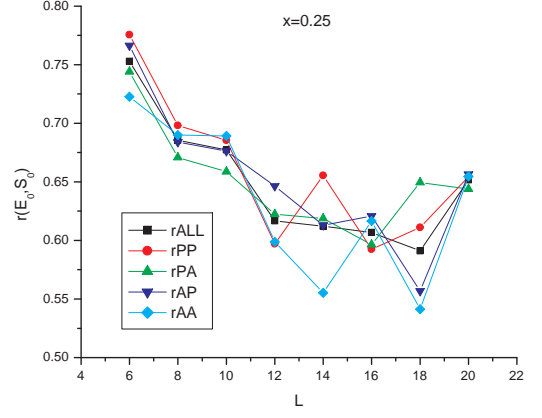


FIG. 6: (color online) Covariance of ground state energy and ground state entropy, $r(E_0, S_0)$ vs. L for $x = 0.25$.

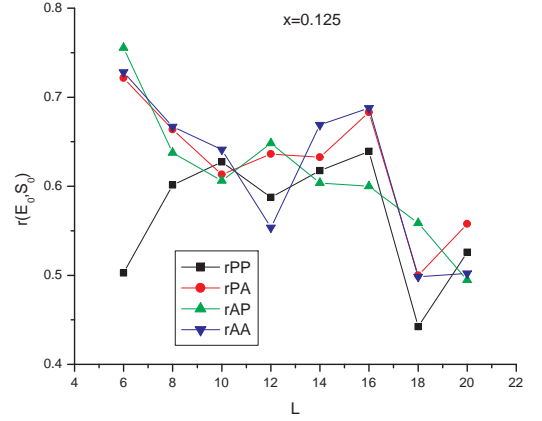


FIG. 7: (color online) Covariance of ground state energy and ground state entropy, $r(E_0, S_0)$ vs. L for $x = 0.125$.

the ensemble in which we fix both the number of negative bonds and the number of frustrated plaquettes for each value of L , one would find higher values of r than what we find here. Crudely, one would expect the values of r in the more tightly specified ensemble to be higher by about a factor of $1/.8$, the inverse of the r -factor for the correlation between E_0 and the number of frustrated plaquettes.

For $x = 0.25$ and $x = 0.5$, as L increases the slope of the regression line through the data given by the least-squares fit appears to rapidly approach a limit of about $m \approx 0.36$. This number is slightly greater than $\ln(2)/2 = 0.34657\dots$. Naively, this means is that, on the average, the GS degeneracy increases by about a factor of two for each additional broken bond, since each broken bond increases the energy by two units. But m is not actually a physical observable, because it depends on our choice

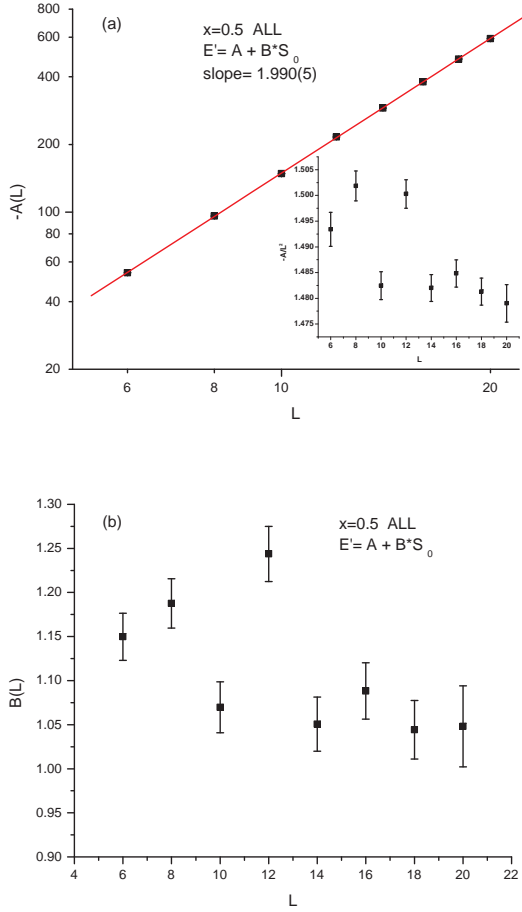


FIG. 8: (color online) Results of least-squares fit analysis parameterized by Eqn. (6) of the scatter plot of correlations between E_0 and S_0 for $x = 0.5$: (a) $-A$ vs. L , log-log plot; inset: $-A/L^2$ vs. L ; (b) B vs. L .

of ensemble. We will say more about what the actual physical quantity is later.

The reader should note that the probability density in the energy-entropy plane shown in Fig. 1(c) is clearly different from a two-dimensional Gaussian distribution, since, with the boundary conditions we are using, E_0 can only have values which are multiples of four units. The previous results in Figure 6 of Landry and Coppersmith,¹⁵ using a much larger number of samples, show that the one-dimensional probability distribution for S_0 at the same values of x and L , which is the projection of the joint distribution onto the entropy axis, can be fit by a Gaussian distribution.

Since it is generally believed that $T = 0$ is a critical point for the model, perhaps what one needs to explain is why the one-dimensional distribution is apparently Gaussian! This result becomes less surprising, however, once one realizes that the strong correlations between E_0 and the number of frustrated plaquettes will make it very

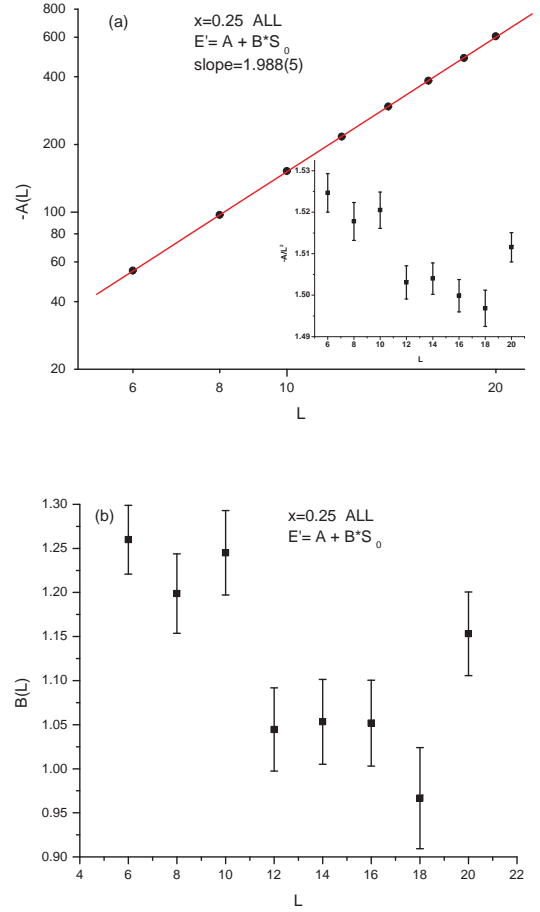


FIG. 9: (color online) Results of least-squares fit analysis parameterized by Eqn. (6) of the scatter plot of correlations between E_0 and S_0 for $x = 0.25$: (a) $-A$ vs. L , log-log plot; inset: $-A/L^2$ vs. L ; (b) B vs. L .

difficult to see any non-Gaussian behavior in this one-dimensional distribution, unless one holds the number of frustrated plaquettes fixed. In our ensemble, the number of frustrated plaquettes always has a Gaussian distribution.

For $x = 0.125$, where the ferromagnetic correlations are substantial¹⁸ for small L , the strength of the energy-entropy correlation is somewhat reduced for the case of periodic boundary conditions in both directions. This effect is probably a result of the fact that for small L at $x = 0.125$, the behavior is essentially dominated by short-range ferromagnetic correlations.

It is equally valid to do the least-squares fit using S_0 as the independent variable. The results of fits of this type for $x = 0.5$, 0.25 and 0.125 , using the same data as before, are shown in Figures 8, 9 and 10, respectively. The values of r are not shown again, since they are unchanged from the earlier case. For each value of x and each L , we now show the slope B of the least-squares fit, and the offset

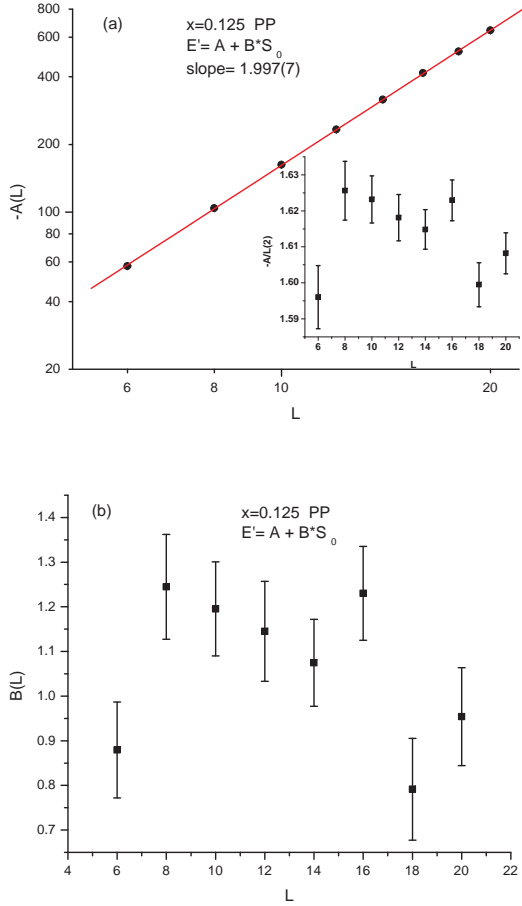


FIG. 10: (color online) Results of least-squares fit analysis parameterized by Eqn. (6) of the scatter plot of correlations between E_0 and S_0 for $x = 0.125$: (a) $-A$ vs. L , log-log plot; inset: $-A/L^2$ vs. L ; (b) B vs. L .

A of the energy, defined by

$$E'(S_0) = A + B * S_0. \quad (6)$$

Now the notation E' indicates that energy is the dependent variable in the least-squares fit. Since A is negative, we use $-A$ in the log-log plot.

From the log-log plots in Figs. 2(a) and 3(a), we find that b is proportional to $L^{1.78(2)}$ and $L^{1.81(4)}$, respectively, while from Figs. 8(a) and 9(a), the scaling of $-A$ is essentially indistinguishable from L^2 . A closer inspection of Fig. 3(a), however, reveals that there is a clear curvature of the data on the log-log plot. We can see in the inset to Fig. 3(a) that, for $x = 0.25$, b becomes essentially proportional to L^2 for $L \geq 12$.

There is no known reason for a qualitative difference in the scaling behavior between $x = 0.5$ and $x = 0.25$. Therefore, we anticipate that the entropy scaling will also become proportional to L^2 for some larger L in the $x = 0.5$ case. Given the results in the literature, we expect that this will happen before L reaches 30.

As we have demonstrated in Fig. 1(c) and 1(d), the regression line which is obtained when one uses S_0 as the independent variable is not the same one which is found by using E_0 as the independent variable. The slope parameters of these two regression lines are related to each other¹⁹ as

$$mB = r^2. \quad (7)$$

Since r^2 is, in general, a number between 0 and 1, we are faced with the problem of deciding what the true best line through the data is. Without some additional information, there is no unique prescription for solving this problem.²⁰

We can write down an equation for the joint probability distribution which builds in the fact that the allowed values of E_0 are quantized:

$$P_L(E_0, S_0) = C_L f\left(\frac{E_0 - \langle E_0(L) \rangle}{\sigma(E_0(L))}, \frac{S_0 - \langle S_0(L) \rangle}{\sigma(S_0(L))}\right) \left[\sum_{n=-\infty}^{\infty} \delta(E_0 - 4n) \right]. \quad (8)$$

The dependence on x is not shown explicitly, and C_L is the normalization constant. Aside from small corrections to scaling which can be ignored for large L , we expect that we can assume

$$\langle E_0(L) \rangle = E_\infty L^2, \quad (9)$$

and

$$\langle S_0(L) \rangle = S_\infty L^2. \quad (10)$$

It should also be safe^{9,15} to assume that $\sigma(E_0(L)) =$

$\bar{\sigma}_E L$. The scaling of $\sigma(S_0(L))$ with L appears to be nontrivial,^{9,15} but we certainly expect that it will diverge as L goes to infinity. Therefore, for large L it should be an adequate approximation to replace the sum over the δ -functions by a uniform background.

If the envelope function f of the probability distribution in the energy-entropy plane was a two-dimensional

Gaussian, then it would have the normal form

$$f_G(X, Y) = \frac{1}{2\pi\sqrt{1-r^2}} \exp\left(-\frac{X^2 - 2rXY + Y^2}{2(1-r^2)}\right), \quad (11)$$

where the arguments X and Y have probability distributions with zero mean and unit standard deviation. Given this assumption, which is unproven, we should treat E_0 and S_0 on an equal basis. Then it would be correct to set the best regression line through the joint probability distribution to be equal to

$$S_0 - S_\infty = (m/r) * (E_0 - E_\infty), \quad (12)$$

or, equivalently,

$$E_0 - E_\infty = (B/r) * (S_0 - S_\infty). \quad (13)$$

As we have repeatedly reminded the reader, $T = 0$ is believed to be a critical point for this model, so the assumption of Gaussian fluctuations can be justified only as an approximation. We do not really know what actual form of $f(X, Y)$ should be used, and therefore^{19,20} we do not know what the slope of the best regression line should be. However, it seems certain that corrections to the Gaussian approximation are invisible at our current level of statistical uncertainty.

IV. DISCUSSION

One might think that the behavior of the A and B parameters which we find by treating the entropy as the independent variable in the least-squares fit are quite simple. It is important to remember, however, that the slope of the best line through the data is *not* B . Within the Gaussian approximation, as we have remarked above, the slope of the best line is B/r . And thus if the slope of the best line through the data is to have some finite slope in the large L limit, it appears necessary to have a finite limit for r .

In Figures 11, 12 and 13, we show the values of B/r vs. L . The value of B/r appears to be approximately independent of L for $x = 0.125$ and 0.25 , because the L dependences of B and r cancel each other, although the statistical uncertainties are too large for precise statements to be made. For $x = 0.5$, however, B/r may be increasing with L within our range of L .

Dimensionally, the slope B/r defined in Eqn. (13) has units of temperature. It is tempting to argue that B/r has some relation to a fictive glass temperature for the crossover between high and low temperature dynamical behavior. Thus, a naive prediction for B/r would be that it should be proportional to the mean-field energy scale, which is

$$E_{mf} = 2\sqrt{x(1-x)}, \quad (14)$$

where the factor of 2 comes from the square root of the number of neighbors on the lattice, and the factor of

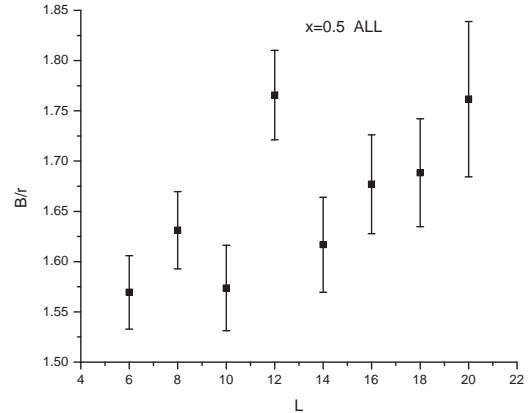


FIG. 11: B/r vs. L for $x = 0.5$.

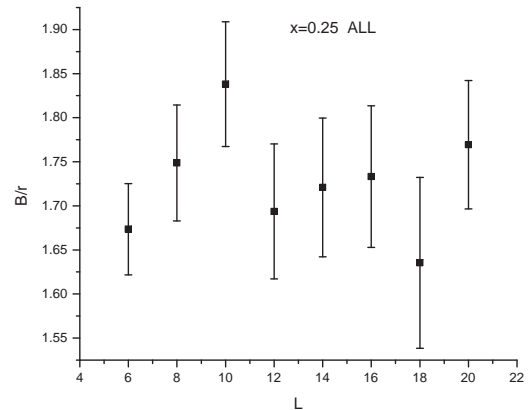


FIG. 12: B/r vs. L for $x = 0.25$.

$x(1-x)$ is the second moment of $P(J_{ij})$. However, no such dependence on x is seen in our data. The value of B/r actually seems to be decreasing slowly as x increases from 0.125 to 0.5. For $x = 0.5$, if we average the data for all L , we find

$$B/r = 1.66 \pm 0.03. \quad (15)$$

This number probably underestimates the result for large L slightly, due to the apparent tendency for B/r to increase with L . The quoted statistical error does not include any allowance for this effect. Using Eqn. (15), however, we find that, on the average, each additional broken bond in the ground state increases the GS degeneracy by a factor of 3.34(7). Our uncertainties for the smaller values of x are larger, but this is primarily because we have smaller numbers of samples for these cases.

For any GS on a square lattice, each spin which has two neighbor spins that are oriented along the direction favored by the bond between them, with the other two neighbor spins pointed opposite to the direction favored

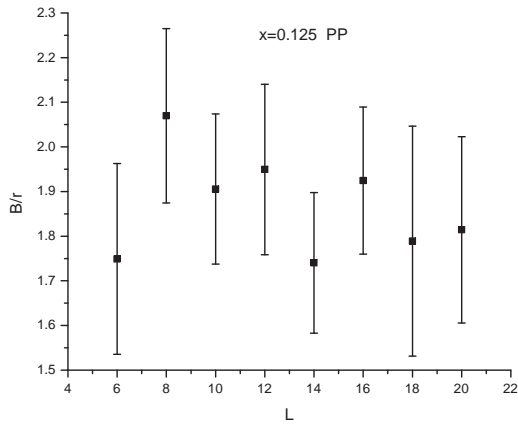


FIG. 13: B/r vs. L for $x = 0.125$.

by the bond (*i.e.* these bonds are broken), can flip with no energy cost. Each of these free spins contributes a factor of two to the degeneracy of the GS. It is thus expected that increasing the number of broken bonds in the GS would also increase the number of such free spins. It is not reasonable, however, that increasing the number of broken bonds by one would increase the number of free spins by nearly two, on the average. Therefore, the fact that we have found the average increase in the GS degeneracy for each additional broken bond to be a factor of about 10/3 indicates that this effect cannot be explained by fluctuations in the number of zero-energy single-spin flips. There must be a substantial contribution from large-scale rearrangements of the GS structure.

An exact calculation of the energy-entropy correlation for $L = 50$, or possibly $L = 60$, could be performed using the method of Galluccio, Loeb, and Vondrák.²¹ It should be noted, however, that it is not really necessary to calculate S_0 exactly. It would be more than sufficient to have an approximate calculation of S_0 which was accurate to one part in 10^4 . That does not seem impossible, and it might allow calculations for even larger L .

An explicit calculation of the low temperature specific heat for $x = 0.5$ by Lukic *et al.*⁶ gives a result proportional to $\exp(-2/T)$ when $L > 30$. It is natural that crossover behavior should be seen in both S_0 and the low T specific heat, with the same crossover length. The low T limit of the specific heat in this model is determined by the degeneracy of the states at energy 4 above the GS. It is surely not surprising that the degeneracies of the ground states and the first excited states would be controlled by the same crossover length. To verify that this is occurring, the calculation of Lukic *et al.* could be repeated for $x = 0.25$. We expect that a crossover length of $L \approx 12$ will be found for the specific heat in that case.

Katzgraber and Lee²² have calculated the T dependence of the correlation length in this model, and found that it behaves as $\exp(2/T)$. (Recall that $J = 1$.) They

use this result to argue that the specific heat at low T should be proportional to $\exp(-4/T)$, as one might naively expect for a model with an energy gap of 4. However, a more detailed analysis²³ has found that their data for the specific heat agree with the conclusions of Lukic *et al.*⁶ Another recent study by Wang,²⁴ using a new algorithm, also finds that the low T specific heat is proportional to $\exp(-2/T)$.

It would also be interesting to repeat these calculations on a hexagonal lattice, where the allowed energy states are multiples of two units, because the number of bonds for each site is odd. Thus on this lattice the smallest zero-energy excitation of the $\pm J$ model involves two neighboring spins. We would expect that the low temperature specific heat is proportional to $\exp(-2/T)$ for the whole range of L in that case.

The analogy to an Ising chain which is made by Wang and Swendsen¹⁶ to argue for a specific heat which is proportional to $\exp(-2/T)$ has nothing to do with random bonds. We know, however, that in 2D a fully frustrated Ising system does not display this behavior.⁹ In addition, by studying triangular lattices, Poulter and Blackman²⁵ found that adding a small concentration of unfrustrated plaquettes to a fully frustrated system does not produce spin-glass behavior.

It was recently shown by Amoruso, Marinari, Martin and Pagnani²⁶ that the behavior of domain wall energies for the 2D Ising spin glass is fundamentally different in those cases, such as the $\pm J$ model, where the energies are quantized. In a very interesting paper, Wang, Harrington and Preskill²⁷ have argued that the presence of an energy gap allows the existence of topological long-range order. A less specific suggestion of topological long-range order in 2D random-bond Ising models was made earlier by Merz and Chalker.²⁸ Numerical results for the properties of domain walls, which will be presented elsewhere,^{29,30} are consistent with this proposal.

What we want to do is to explain the low temperature behavior of the specific heat in terms of topological excitations. We know that in the spin-glass region of the phase diagram it is difficult to find a way to overturn a finite fraction of a large sample at zero energy cost. In contrast, at and near the fully frustrated system, where the $\exp(-2/T)$ behavior of the specific heat does not occur, it becomes easy to find ways of overturning a finite fraction of the spins at zero energy cost. This explains the difference between the spin-glass region and the fully frustrated region.

What is possible in the spin-glass region is finding many ways of overturning a finite fraction of the large sample at a cost of only 4.²⁹ This is precisely the generalization of the Wang-Swendsen mechanism¹⁶ to a random 2D system. And because we can do this, the behavior of the Parisi overlap function³¹ will be nontrivial. Of course, since T_c is zero, the overlap function collapses to zero as L increases. But if we scale out this simple collapse with L , the existence of the large-scale finite-energy excitations may be observed in the overlap function. Since we

are trying to observe effects caused by states of energy $4J$, we cannot merely do a naive $T = 0$ calculation of the overlap function. However, by manipulating the double limit $L \rightarrow \infty$ and $T \rightarrow 0$, it may be possible to see the effect.

Although the actual implementation would be very challenging, one can imagine studying the energy-entropy correlation at and below T_c in a three-dimensional Ising spin glass, using thermal-average values for the energy and entropy. In that case, where the spin-glass phase and the failure of self-averaging of the Parisi overlap function are believed to occur at finite T ,³² one can use a general probability distribution for $P(J_{ij})$ and still have a positive entropy, in contrast to the 2D situation.

The author's expectation is that the anomalous scaling which we find for the $\pm J$ model at $T = 0$ in 2D for small L will occur for all types of bond distributions in 3D, where the spin-glass transition is at $T > 0$. It might also happen that the crossover length becomes infinite in 3D, but it seems more likely that the crossover length is only infinite in four or more dimensions.

V. SUMMARY

We have found that for $L \times L$ square lattices with $L \leq 20$ the 2D Ising spin glass with $+1$ and -1 bonds has a very strong correlation between E_0 and the number of frustrated plaquettes, and, what is more surprising, a strong correlation between E_0 and S_0 . On the average,

each additional broken bond in the GS of a particular sample of random bonds increases the GS degeneracy by a factor of about $10/3$. This number is too large to be explained by fluctuations in the number of free spins, which implies that there is a substantial contribution due to large-scale rearrangements of the GS structure. Over this range of L , the characteristic GS entropy scales as $L^{1.78(2)}$ for $x = 0.5$, while the characteristic GS energy scales as L^2 , as expected. For $x = 0.25$, however, a crossover is seen to normal scaling behavior of S_0 near $L = 12$. We believe that a similar crossover will occur for $x = 0.5$ at $L \approx 25$, and that this crossover is connected to the anomalous behavior of the low temperature specific heat. We explain why the Wang-Swendsen mechanism for a low T specific heat proportional to $\exp(-2/T)$ should apply in the spin-glass regime, but not in the fully frustrated regime.

Acknowledgments

The author thanks S. N. Coppersmith for generously providing all of the raw data analyzed in this work, and for a careful reading of an early version of the manuscript. The computer program used by Prof. Coppersmith to generate the data was written by J. W. Landry, and is an adaptation of the code written by L. Saul. The author is grateful to S. L. Sondhi, F. D. M. Haldane, A. K. Hartmann and H. G. Katzgraber for helpful discussions, and to Princeton University for providing use of facilities.

* ron@princeton.edu

- ¹ S. F. Edwards and P. W. Anderson, J. Phys. F **5**, 965 (1975).
- ² J. A. Blackman and J. Poulter, Phys. Rev. B **44**, 4374 (1991).
- ³ J. A. Blackman, J. R. Goncalves and J. Poulter, Phys. Rev. E **58**, 1502 (1998).
- ⁴ J. Houdayer, Eur. Phys. J. B **22**, 479 (2001).
- ⁵ A. K. Hartmann and A. P. Young, Phys. Rev. B **64**, 180404(R) (2001).
- ⁶ J. Lukic, A. Galluccio, E. Marinari, O. C. Martin and G. Rinaldi, Phys. Rev. Lett. **92**, 117202 (2004).
- ⁷ I. A. Campbell, A. K. Hartmann and H. G. Katzgraber, Phys. Rev. B **70**, 054429 (2004).
- ⁸ L. Saul and M. Kardar, Phys. Rev. E **48**, R3221 (1993).
- ⁹ L. Saul and M. Kardar, Nucl. Phys. B **432**, 641 (1994).
- ¹⁰ T. Shirakura and F. Matsubara, J. Phys. Soc. Jpn. **65**, 3138 (1996).
- ¹¹ F. Matsubara, T. Shirakura and M. Shiomi, Phys. Rev. B **58**, R11821 (1998).
- ¹² M. Shiomi, F. Matsubara and T. Shirakura, J. Phys. Soc. Jpn. **69**, 2798 (2000).
- ¹³ N. Hatano and J. E. Gubernatis, Phys. Rev. B **66**, 54437 (2002).
- ¹⁴ R. Fisch, Phys. Rev. B **51**, 11507 (1995).
- ¹⁵ J. W. Landry and S. N. Coppersmith, Phys. Rev. B **65**, 134404 (2001).

- ¹⁶ J.-S. Wang and R. H. Swendsen, Phys. Rev. B **38**, 4840 (1988).
- ¹⁷ ©OriginLab Corporation, Northampton, MA 01060.
- ¹⁸ C. Amoruso and A. K. Hartmann, Phys. Rev. B **70**, 134425 (2004).
- ¹⁹ J. W. Tukey, Biometrics **7**, 33 (1951).
- ²⁰ A. Madansky, J. Am. Stat. Assoc. **54**, 173 (1959).
- ²¹ A. Galluccio, M. Loebl and J. Vondrák, Phys. Rev. Lett. **84**, 5924 (2000).
- ²² H. G. Katzgraber and L. W. Lee, Phys. Rev. B **71**, 134404 (2005).
- ²³ H. G. Katzgraber, L. W. Lee and I. A. Campbell, cond-mat/0510668.
- ²⁴ J.-S. Wang, Phys. Rev. E **72**, 036706 (2005).
- ²⁵ J. Poulter and J. A. Blackman, J. Phys. A **34**, 7527 (2001).
- ²⁶ C. Amoruso, E. Marinari, O. C. Martin and A. Pagnani, Phys. Rev. Lett. **91**, 087201 (2003).
- ²⁷ C. Wang, J. Harrington and J. Preskill, Ann. Phys. (N.Y.) **303**, 31 (2003).
- ²⁸ F. Merz and J. T. Chalker, Phys. Rev. B **66**, 054413 (2002).
- ²⁹ R. Fisch, cond-mat/0508468.
- ³⁰ R. Fisch and A. K. Hartmann, cond-mat/0603729.
- ³¹ G. Parisi, Phys. Rev. Lett. **50**, 1946 (1983).
- ³² M. Palassini, M. Sales and F. Ritort, Phys. Rev. B **68**, 224430 (2003).